

Solution of Euler-Bernoulli Beam Equation by Integral Transform Method

Jonathan K. Black, Josh Blackham

Mechanical Engineering Department
Brigham Young University
Provo, Utah 84602
jblack42@byu.edu, jeb419@byu.edu

Abstract

The Euler-Bernoulli beam theory is a simple model for small lateral deflections in beams. This work derives the solution to the Euler-Bernoulli equation using the generalized finite integral transform method. The eigenvalue problem is considered to find eigenfunctions, which are used to define an integral transform, which, along with the Laplace transform, is used to solve the PDE. The solution is then evaluated numerically, simulating the response of a cantilevered beam to various time-varying point sources. Mode shapes of the cantilevered beam are shown to be excited by a sinusoidal input near the modal resonant frequency, with a superposition of modes also being observed in the swept sine and impact simulations.

Nomenclature

u	solution to Euler-Bernoulli beam equation
E	elastic modulus of beam material
I	second moment of area
ρ	linear density
q	distributed load
L	length of beam
x_0	location of point source
ω_s	frequency of point source
μ	eigenvalues of supplementary problem

Introduction

Deriving and solving partial differential equations that model beam vibrations accurately is an important and useful skill when looking to model a system. Partial differential equations are an effective tool for modeling high frequency responses and in determining parameters for modal analysis. Analytical functions that express these modal properties of simple systems can act as a guide or benchmark in testing or in approximate simulation. Despite this, the complexity and difficulty of finding solutions to partial differential equations increases greatly as more complex systems are considered. Cross-sections that are not constant, supports that are not at the ends of the beam, or analyses of curved bars, plates or shells become quite difficult to model [1].

The Euler-Bernoulli Beam theory is the basis for analysis of extensional and flexural motion, while ignoring torsional motion. It is useful for very basic beam bending analyses and provides useful insight for responses of beams under different loading conditions [1].

Problem Description

In [1], the equation of motion for flexural vibration of a beam according to Euler-Bernoulli beam theory is given

as

$$\frac{\partial^2}{\partial x^2} \left(EI \frac{\partial^2 u}{\partial x^2} \right) = -\rho \frac{\partial^2 u}{\partial t^2} + q \quad (1)$$

where E is the elastic modulus, I is the second moment of area (a.k.a. area moment of inertia), ρ is the linear density, and q is the distributed load as a function of x and t .

This work will assume a homogeneous, constant cross section beam, so that the equation simplifies as follows:

$$EI \frac{\partial^4 u}{\partial x^4} = -\rho \frac{\partial^2 u}{\partial t^2} + q \quad (2)$$

The beam is initially undergoing no deflection and is at rest.

$$u(x, 0) = \frac{\partial u}{\partial t}(x, 0) = 0$$

The beam is cantilevered; in other words, one end is fixed and the other end is free. The first end being fixed implies two geometric boundary conditions: deflection and slope must be zero at the wall. The free end has no geometric boundary conditions imposed, but two natural boundary conditions arise from the recognition that the free end has no applied moments or shear loads. Because internal moment and shear are proportional to the second and third derivatives of deflection, respectively, those derivatives must be zero at the free end [1]. These four boundary conditions can be stated mathematically as follows:

$$\begin{aligned} u(0, t) &= \frac{\partial u}{\partial x}(0, t) = 0 \\ \frac{\partial^2 u}{\partial x^2}(L, t) &= \frac{\partial^3 u}{\partial x^3}(L, t) = 0 \end{aligned}$$

For our exploration of the solution we allow q to be a point source. We consider the following three different forcing conditions:

$$\begin{aligned} q_1(x, t) &= \delta(x - x_0)\delta(t) \\ q_2(x, t) &= \delta(x - x_0)\sin(\omega_s t) \\ q_3(x, t) &= \delta(x - x_0)\sin(\omega_s(t)t) \end{aligned} \quad (3)$$

where ω_s is a constant in q_2 and $\omega_s(t)$ is an arbitrary function of time in q_3 .

Eigenvalue Problem

We now solve the eigenvalue problem for the Euler-Bernoulli equation in order to find the eigenvalues and

eigenfunctions. We first consider the supplementary eigenvalue problem

$$\frac{d^4 X}{dx^4} = \mu X$$

Assuming $X = e^{\lambda x}$ and solving the auxiliary equation for λ gives

$$\begin{aligned} \lambda^4 &= \mu \\ \lambda &= \pm \sqrt[4]{\mu}, \pm i \sqrt[4]{\mu} \end{aligned}$$

The general solution can now be written as follows:

$$\begin{aligned} X(x) &= c_1 \cosh(\lambda x) + c_2 \sinh(\lambda x) \\ &+ c_3 \cos(\lambda x) + c_4 \sin(\lambda x) \end{aligned} \quad (4)$$

Using the boundary conditions at $u(0, t)$, we are able to find the following relations:

$$\begin{aligned} c_1 &= -c_3 \\ c_2 &= -c_4 \end{aligned}$$

We then simplify Equation 4 and use one of the boundary conditions at $u(L, t)$ to find the relation β described below. We recognize that any scalar multiple of an eigenfunction is still an eigenfunction and result in the following:

$$\begin{aligned} X(x) &= \cosh(\lambda x) - \cos(\lambda x) \\ &- \beta(\sinh(\lambda x) - \sin(\lambda x)) \end{aligned} \quad (5)$$

where

$$\beta = \frac{\cosh(\lambda L) + \cos(\lambda L)}{\sinh(\lambda L) + \sin(\lambda L)}$$

From the fourth boundary condition, it is found that the eigenvalues λ must satisfy the following equation:

$$1 + \cos(\lambda L)\cosh(\lambda L) = 0 \quad (6)$$

This function is plotted in Figure 1. It can be seen that there are infinitely many roots, as expected. The λ values that satisfy Equation 6 will hereafter be denoted λ_n , and the corresponding eigenfunctions (according to Equation 5) will be denoted X_n .

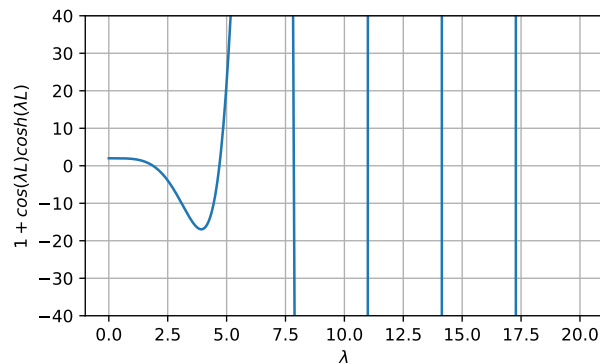


Figure 1: Plot of the function used to solve for eigenvalues

The first 4 eigenfunctions can be seen in Figure 2 and are the normal modes, or mode shapes, of the vibrating cantilever beam. In [1], it was shown that the eigenfunctions of this eigenvalue problem are orthogonal as long as boundary conditions for both ends are either fixed or free.

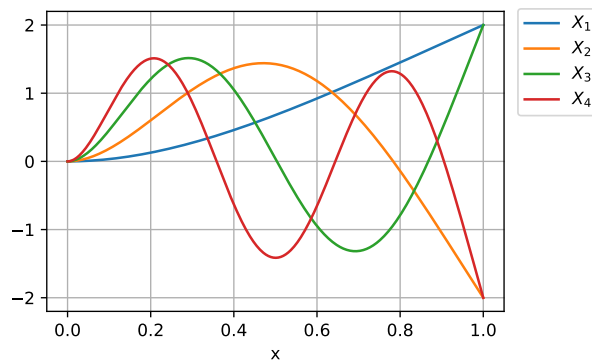


Figure 2: Plot of the first 4 eigenfunctions, normalized by the square of their norm.

Finite Integral Transform

The eigenfunctions X_n will be used to define a generalized finite integral transform, which will later be used to eliminate the fourth derivative in the Euler-Bernoulli beam equation.

Assuming a weight function of $p(x) = 1$, the inner

product and norm can be defined as follows:

$$(v, w) = \int_0^L v(x)w(x)dx$$

$$\|v(x)\|^2 = (v, v) = \int_0^L v^2(x)dx$$

With the inner product defined, the vector space $L^2(0, L)$ is a Hilbert space and the eigenfunctions $X_n(x)$ from equation 5 can be used as a basis set for a generalized Fourier series:

$$v(x) = \sum_{n=1}^{\infty} \frac{(v, X_n)}{\|X_n\|^2} X_n \quad (7)$$

The integral transform and its inverse are now defined as follows:

$$\mathcal{T}\{v(x)\} = (v, X_n) = \int_0^L v(x)X_n(x)dx = \bar{v}_n \quad (8)$$

$$\mathcal{T}^{-1}\{\bar{v}_n\} = \sum_{n=1}^{\infty} \bar{v}_n \frac{X_n(x)}{\|X_n\|^2} = v(x) \quad (9)$$

Operational Property

The operational property of the integral transform must be derived to determine the effect of applying it to the 4th order partial derivative, which is the main differential operator in the Euler-Bernoulli beam equation.

We apply the integral transform to the 4th order partial derivative term of the Euler-Bernoulli equation.

$$\mathcal{T}\left\{\frac{\partial^4 u}{\partial x^4}\right\} = \int_0^L \frac{\partial^4 u}{\partial x^4} X_n dx$$

After performing integration by parts multiple times and applying the boundary conditions, we have the following:

$$\mathcal{T}\left\{\frac{\partial^4 u}{\partial x^4}\right\} = \int_0^L u \frac{d^4 X_n}{dx^4} dx$$

We solve for the 4th derivative of the eigenfunction.

$$\begin{aligned} \frac{d^4 X_n}{dx^4} &= \lambda_n^4 (\cosh(\lambda_n x) - \cos(\lambda_n x)) \\ &\quad - \beta_n (\sinh(\lambda_n x) - \sin(\lambda_n x)) = \lambda_n^4 X_n \end{aligned}$$

We can now simplify the integral further, using the definition of the integral transform (Equation 8).

$$\mathfrak{I} \left\{ \frac{\partial^4 u}{\partial x^4} \right\} = \int_0^L u \frac{d^4 X_n}{dx^4} dx = \int_0^L \lambda_n^4 u X_n dx = \lambda_n^4 \bar{u}_n \quad (10)$$

Solution of Euler-Bernoulli Equation

Now that the operational property has been defined for the 4th order derivative, we apply the finite integral transform. We begin with the Euler-Bernoulli equation.

$$EI \frac{\partial u}{\partial x^4} = -\rho \frac{\partial u}{\partial t^2} + q$$

We first apply the generalized integral transform, \mathfrak{I} , to the function and initial conditions (which are zero).

$$EI \lambda_n^4 \bar{u}_n = -\rho \frac{\partial \bar{u}_n}{\partial t^2} + \bar{q}_n$$

We next apply the Laplace transform, denoting $\mathfrak{L}\{v\} = \hat{v}$.

$$EI \lambda_n^4 \hat{u}_n = -\rho s^2 \hat{u}_n + \hat{q}_n$$

We solve for the transformed solution, \hat{u}_n .

$$\hat{u}_n = \frac{\hat{q}_n}{EI \lambda_n^4 + \rho s^2}$$

We now apply the inverse Laplace transform, \mathfrak{L}^{-1} , using the convolution theorem.

$$\begin{aligned} \bar{u}_n &= \bar{q}_n * \frac{1}{\rho \omega_n} \sin(\omega_n t) \\ \omega_n &= \lambda_n^2 \sqrt{\frac{EI}{\rho}} \end{aligned} \quad (11)$$

Finally, we apply the inverse finite integral transform, \mathfrak{I}^{-1} (Equation 9).

$$u = \sum_{n=1}^{\infty} \bar{u}_n \frac{X_n}{\|X_n\|^2} \quad (12)$$

Implementation

A Python script was developed to implement eqs. (6), (11) and (12) and to create animations of the response of the beam to various forcing functions, $q(x, t)$.

To improve performance, every factor in the summation in Equation 12 was pre-calculated and stored, instead of re-calculating \bar{u}_n , X_n , and $\|X_n\|^2$ at every combination of n , x , and t . This resulted in two rank 2 tensors: \bar{u}_{nt} and \tilde{X}_{nx} , where \tilde{X} represents an eigenvector normalized by the square of its norm. In these expressions, x and t represent indices in discretized space and time vectors instead of continuous variables. Once these two tensors were calculated, all that remained was to perform the summation, which is re-written using Einstein tensor summation notation as follows:

$$u_{xt} = u_{nt} \tilde{X}_{nx} \quad (13)$$

For the simpler forcing functions, q_1 and q_2 , the convolution integral in Equation 11 was evaluated analytically. For the forcing function with time varying frequency, q_3 , the convolution integral was evaluated numerically using the adaptive quadrature method *scipy.integrate.quad*.

Results

All results presented use the parameters $EI = 1$, $L = 1$, and $\rho = 1$.

The first four roots of Equation 6 and the corresponding natural frequencies ω_n are presented in Table 1.

n	λ_n	ω_n
1	1.8751	3.5160
2	4.6941	22.0345
3	7.8548	61.6972
4	10.9955	120.9019

Table 1: Eigenvalues and natural frequencies of the first 4 modes.

We successfully simulated the response of the beam to all three loading conditions described in Equation 3. All of the animations can be found in the GitHub repository, as presented in the Supplementary Files section.

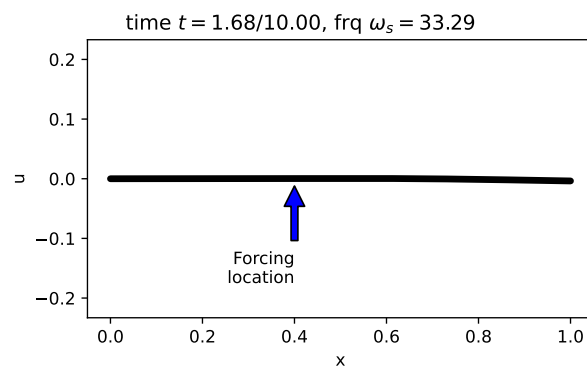


Figure 3: A frame from the swept sine excitation simulation, with ω_s well above the natural frequencies of modes 1 and 2, which fails to excite any mode significantly.

First, we will discuss the results of a swept sine animation, where the time-varying frequency is given by $\omega_s = 40 - 4t$ and the simulation was carried out with $t \in [0, 10]$ such that all frequencies between 40 and 0 are reached. For the first 2 seconds of the simulation, when the source frequency is above 30, almost no response is seen (see Figure 3), which is to be expected because there are no modes that resonate near those frequencies.

As the forcing frequency nears the resonant frequency of the second mode, however, the animation displays behavior dominated by the second mode shape (see Figure 4 and compare Figure 2).

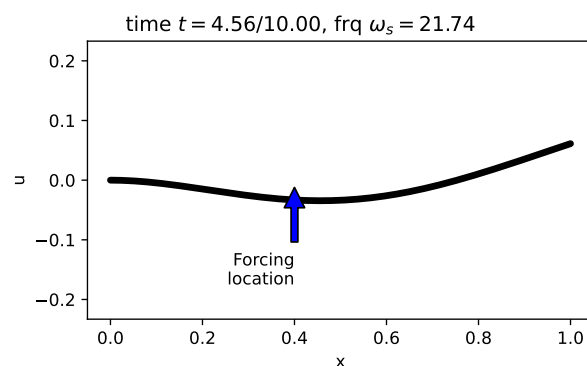


Figure 4: A frame from the swept sine excitation simulation, with ω_s near the natural frequency of mode 2. Compare this shape with X_2 from Figure 2.

Later, as the source frequency continues to drop, we see a superposition of modes 1 and 2 (see Figure 5), as the energy that was put into mode 2 has no way of being dissipated since no damping terms were included in our model.

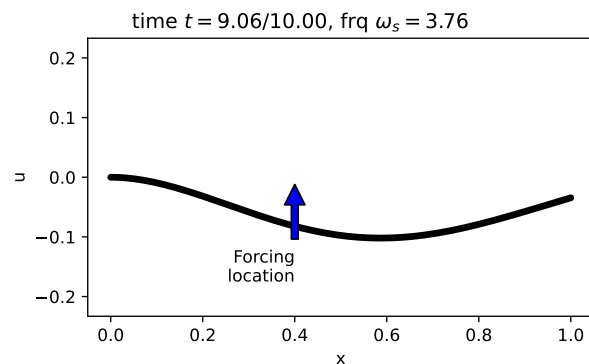


Figure 5: A frame from the swept sine excitation simulation, with ω_s near the natural frequency of mode 1. Note the superimposed behavior of modes 1 and 2 (see X_1 and X_2 from Figure 2).

The impulse input, q_1 , was used to explore the effect of excitation position, x_0 . An impulse imparts energy at every frequency (the Fourier transform of a delta function is a constant), so we expect every mode to be excited, unless the impulse is placed at the node of the mode. To observe this behavior, an impulse was applied at the node of mode 2, which is $x_0 = 0.7834$. One frame from that simulation is shown in Figure 6. As expected, the response included mode 1 and many higher frequency modes, but did not include the mode 2 behavior.

Conclusions

The solutions found for the Euler-Bernoulli equation are able to accurately show the mode shapes and frequencies of the modeled cantilever beam. We also reasonably model the response of the cantilever beam to the different forcing functions and are able to see the interactions of mode shapes due to the impact and throughout the swept sine. Future work may include building on the three input functions to simulate other and more complicated inputs, and investigation on modal interactions due to various in-

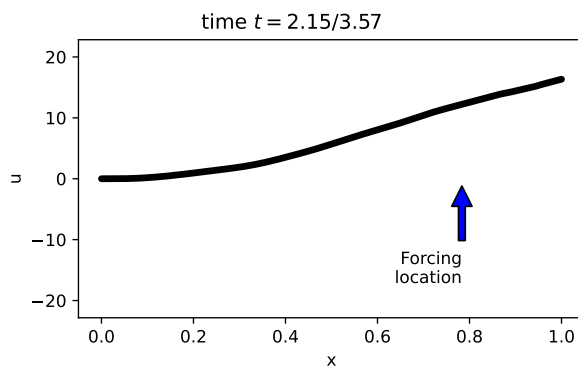


Figure 6: A frame from the impulse excitation simulation with the input being placed at the node of mode 2. Observe the superimposed mode shapes of several modes, most noticeably modes 1 and 3.

puts. The model could also be updated to include other boundary conditions or damping terms to more accurately model a wider range of real structures.

Acknowledgements

Dr. Vladimir Soloviev greatly helped with the derivation of the operational property and explaining the principles of the generalized finite integral transform method.

References

- [1] Jerry H. Ginsberg. *Mechanical and Structural Vibrations*. 1st ed. 2001.

Supplementary Files

The Python code, together with figures and animations, is hosted on GitHub: https://github.com/jonkb/beam_EB.